NASA Technical Paper 3126

# Effect of Crash Pulse Shape on Scat Stroke Requirements for Limiting Loads on Occupants of Aircraft

*Huey D. Carden*

February 1992

## Summary

An analytical study was made to (1) provide comparative information on various crash pulse shapes that potentially could be used to test seats to the parameter conditions included in Federal Regulations Part 23 § 23.562(b)(1) for dynamic testing of general aviation seats, (2) show the effects that crash pulse shape can have on the seat stroke requirements necessary to maintain a specified limit loading on the seat/occupant under various *vertical* crash pulse loadings, (3) compare results from certain analytical model pulses with approximations of actual crash pulses, and (4) compare analytical seat results from application of the specified test parameters of the seat test regulation with experimental airplane crash data. Equations for five models of potentially useful pulse shapes were derived which express the displacement of the aircraft structure and the displacement of the seat/occupant in terms of the maximum deceleration, velocity change, limit seat pan load, and pulse time. From these equations, analytical seat stroke data were obtained under the test conditions as specified in Federal Regulations Part 23 § 23.562(b)(1) for dynamic testing of general aviation seats.

## Introduction

With the advent of transportation vehicles came sometimes unwanted application of suddenly applied accelerations to human occupants of such vehicles. Abnormal accelerations, for example, arise in airplanes from the impact of the vehicle with the ground during a crash. Research in aviation crash dynamics dates back to the pioneering work of Hugh De Haven in the 1940's. De Haven survived a midair collision and the ensuing crash of an airplane to later initiate crash research through on-site investigations of aircraft accidents to identify components and subsystems which contributed to injury and fatality. Results from this work produced design guidelines that remain pertinent today (ref. 1) and can still be found in production of agricultural airplanes (refs. 2 and 3).

Efforts to appraise the hazards of these accelerations to humans are found in reference 4. From this and other literature, it is apparent that whole-body human tolerance to sudden acceleration depends upon many factors, such as (1) direction of acceleration application, (2) magnitude of the acceleration, (3) duration of the acceleration, (4) onset rate of the acceleration, and (5) how the occupant's body is supported during application of the acceleration. Furthermore, various parts of the human body are able to withstand different magnitude and duration of acceleration prior to sustaining injury. For example, accelerations perpendicular to the spine of between $30g$ (0.15-sec duration) and $40g$ (0.05-sec duration) were tolerated by well-restrained human subjects compared with between $5g$ (0.15-sec duration) and $15g$ (0.05-sec duration) for an acceleration applied along the spine (ref. 4). Consequently, when tolerance to crash loads of human subjects in the general population is discussed, often a vertical (along the spine) $g$ load of about $12g$ to $15g$ with a duration of approximately 0.10 sec is mentioned. However, in recent years, the emphasis has shifted to a measure of spinal *load* in the pelvic region of a 49 CFR (Code of Federal Regulations) Part 572 dummy which is considered more meaningful than a $g$ load for assessing the consequences of crash loads on humans.

One means of providing a degree of protection to passengers in aircraft during a crash situation is the seat/restraint system. Various studies have addressed concepts to enhance survivability in crash situations through a load-limiting seat which provides stroking distance under reduced and controlled loads (refs. 5 to 12). Additionally, guidelines for dynamic testing of general aviation seats, which were proposed by the General Aviation Safety Panel (GASP) (ref. 13) and subsequently placed into Federal Regulations (ref. 14), are intended to achieve some degree of occupant protection in crash situations. Specifically, one of the regulations relative to dynamic tests of aircraft seat/restraint systems given by § 23.562(b)(1) states, "For the first test, the change in velocity may not be less than 31 feet per second. The seat/restraint system must be oriented in its nominal position with respect to the airplane and with the horizontal plane of the airplane pitched up 60 degrees, with no yaw, relative to the impact vector. For seat/restraint systems to be installed in the first row of the airplane, peak deceleration must occur in not more than 0.05 sec after impact and must reach a minimum of $19g$. For all other seat/restraint systems, peak deceleration must occur in not more than 0.06 sec after impact and must reach a minimum of $15g$."

Compliance criteria covering all the regulations are included in reference 14; however, the focus of this paper is § 23.562(7) which states, "The compression load measured between the pelvis and lumbar spine of the ATD may not exceed 1500 pounds." (ATD designates anthropomorphic test dummy.) As noted in reference 15, experimental crush data for vertebrae (T8 through T12 and L1 through L5) indicate that the crushing force ranged from slightly over 1300 to 2360 lb. The T9 thoracic vertebrae of the spine (carrying 60 lb which is the estimated upper body weight of a 50-percentile man) was crushed at approximately 1500 lb. Based upon this and other considerations (for example, ref. 16), the criterion became 1500 lb.

Since the regulations in Part 23 do not specify any particular pulse shape to achieve the required magnitudes and durations of the seat loadings in a laboratory environment, the purpose of this paper is to (1) provide comparative information for various pulse shapes that potentially could be used to test seats to meet the regulation, (2) show the effects that crash pulse shape can have on the seat stroke requirements necessary to maintain a specified limit loading on the seat/occupant under various *vertical* crash pulse loadings, (3) compare results from certain analytical model pulses with the approximations of actual crash pulses, and (4) compare the specified test parameters of the regulation to airplane crash test data.

## Symbols

| | |
|---|---|
| $a$ | deceleration, ft/sec$^2$ |
| $a_s$ | deceleration of seat/occupant, ft/sec$^2$ |
| ATD | anthropomorphic test dummy |
| DRI | dynamic response index |
| $g$ | acceleration due to gravity, ft/sec$^2$ |
| $G_l$ | limit deceleration on seat pan, $g$ units |
| $G_m$ | maximum deceleration magnitude of crash pulse, $g$ units |
| $k$ | stiffness of dynamic response index model, lb/ft |
| $K$ | ratio of seat pan limit deceleration to maximum deceleration magnitude of pulse, $G_l/G_m$ |
| $m$ | mass, slugs |
| $S$ | seat stroke, $(S_S - S_A)12$, in. |
| $S_A$ | displacement of airframe, ft |
| $S_S$ | displacement of seat/occupant, ft |
| $t$ | time, sec |
| $t_f$ | maximum duration of seat pan loading, sec |
| $t_L$ | time to reach seat pan maximum deceleration, sec |
| $t_m$ | maximum pulse duration of trapezoidal, skewed or symmetric triangle, and quarter-sine crash pulses (one-half pulse duration or rise time of half-sine crash pulse), sec |
| $t_r$ | rise time to peak deceleration (skewed, or symmetric triangle or trapezoidal pulse), sec |
| $V$ | velocity, ft/sec |
| $V_A$ | velocity of airframe during crash pulse, ft/sec |
| $V_o$ | initial impact velocity, ft/sec |
| $V_S$ | velocity of seat/occupant during crash pulse, ft/sec |
| $V_{S,1}$ | velocity of seat/occupant at time $t_L$ in crash pulse, ft/sec |
| $V_{S,2}$ | velocity of seat/occupant between times $t_L$ and $t_f$ in crash pulse, ft/sec |
| $\ddot{Z}$ | peak of input acceleration for dynamic response index model, $g$ units |
| $\delta_m$ | maximum displacement of dynamic response index model, ft |
| $\Delta t$ | pulse duration of acceleration applied to dynamic response index model, sec |
| $\omega_n$ | natural frequency of dynamic response index model, rad/sec |
| $\zeta$ | damping coefficient of dynamic response index model |

## Analysis

The photographic sequence in figure 1 illustrates the crash dynamics of a general aviation type, single-engine airplane test specimen. The nose landing gear of the airplane specimen contacted the impact surface with an initial velocity, flight-path angle, pitch, roll, and yaw angle. High-speed motion pictures of the crash show the nose gear starting to collapse and the engine cowling contacting the impact surface 0.028 sec after initial ground contact, followed by the starboard wing tip at 0.035 sec. The windshield began to deflect and the fire wall started to penetrate the cabin at 0.060 sec. At the same time, the aft section of the fuselage began to deform, and the starboard landing gear contacted the impact surface. The port landing gear contacted the impact surface at 0.13 sec into the impact, and the port wing immediately thereafter broke away from the fuselage at the aft spar and rotated forward around the front spar.

The approximate pitch attitude was retained during crash impact. At 0.15 sec, the aft cabin section pitched forward about 10° as a result of main landing-gear springback. The airplane then settled back to an angle of about 45° and continued to skid before stopping. The fuselage cabin remained at about the same pitch, roll, and yaw angles as at the initial impact attitude. Obviously, as indicated by the discussion of the sequence of figure 1, a crash is a complex occurrence with a variety of parameters contributing to the airframe load during impact. Aerodynamic, elastic, and plastic structural deformation; inertial forces; and frictional forces interplay to remove the kinetic energy of the airplane and to change the path of the airplane from the conditions just prior to impact. As these events occur, seats and occupants respond to the loads and motions of the crash.

Assumptions and idealizations are made concerning the crash event and the behavior of the seat/occupant and aircraft structure. Under these assumptions and idealizations, equations are presented for the aircraft structural stroke (crushing) and the seat/system displacement as a function of the change in vertical impact velocity for various total pulse durations and pulse shapes where the seat limit design load has been chosen as $12g$. Included in the crash load pulse information are test pulses which could satisfy conditions for testing of general aviation seats as proposed by the General Aviation Safety Panel (GASP) (ref. 13) and could be subsequently included in Federal Regulations Part 23—Airworthiness Standards (ref. 14), hereinafter called Part 23.

In this section, equations are derived for (a) the crushing distance of aircraft structure which would be necessary to produce the idealized crash pulse shapes and (b) the displacement of the seat/occupant system. With these equations, the required stroke of the seat relative to the aircraft that would be necessary to maintain a limit $12g$ load on the seat pan of the seat/occupant undergoing the *vertical* loading of the particular crash pulse can be determined. It is again emphasized that Federal Regulations Part 23 specifies a maximum load (as opposed to a $g$ limit) in the pelvis of an ADT of 1500 lb. The $12g$ seat pan limit is discussed relative to the 1500-lbf criteria and an often used technique for evaluating occupant response to dynamic inputs, the dynamic response index (DRI). The DRI is a one-degree-of-freedom, damped, spring mass model of the upper torso (spine) derived from Air Force experiments (ref. 15). The index is the maximum acceleration response in $g$ units to inputs to the spinal model which has a natural frequency of 52.9 rad/sec and damping ratio of 0.224.

### Assumptions and Idealizations

The crash event of an aircraft as depicted in figure 1 is generally a very complex sequence of events, but a good understanding of the structural response and seat/occupant behavior can be obtained by simplifying analytical techniques. Knowledge of the limitations and assumptions of the analyses is required. Useful trends and typical phenomena associated with the crash event may be studied successfully with such techniques.

Figure 2 presents the various assumed and idealized analytical models of the crash loadings for which required seat stroke distance for maintaining a limit load on the seat pan has been derived. The idealized shapes include

- Trapezoidal pulse (fig. 2(a))
- Half-sine wave (fig. 2(b))
- Quarter-sine wave (fig. 2(c))
- Skewed triangular pulse (fig. 2(d))
- Symmetric triangular pulse (fig. 2(e))

In the derivation of equations for the analytical models of the crash loading pulses, the vertical and longitudinal behavior is assumed to be uncoupled; that is, the influence of longitudinal loads on vertical loads is not considered in any of the equations or data presented. The seat/occupant combination is assumed to follow the structure loading up to the limit load of the seat pan, and no dynamic overshoot is considered in the behavior of the seat pan response. The total vertical impact velocity is assumed to be removed at the end of the crash pulse, and the seat/occupant velocity is also assumed to be reduced to zero at the end of the seat pan limit loading pulse duration. No assumptions are made concerning the availability of actual crushable aircraft structure necessary to produce the crash pulses under consideration nor what seat mechanism could provide the stroking distances.

Appropriate equations derived in the section "Trapezoidal Pulse Load" and the equations presented in the appendix for the other pulse shapes were solved with a commercial computer program on a personal computer. The solutions provided deceleration and seat stroke data for the plots presented in the section "Results and Discussion."

### Trapezoidal Pulse Load

In this section, equations are derived for the trapezoidal pulse loading shape that provides the necessary magnitude, rise time to peak loading, and velocity change specified by Federal Regulations Part 23 for dynamic seat testing (ref. 14.). A detailed derivation is presented only for the trapezoidal pulse shape (sketch A). In the appendix only the equations are given for the other pulse shapes. Results using the equations for these pulse shapes are presented as plots of deceleration versus velocity change and seat stroke in the section "Results and Discussion."

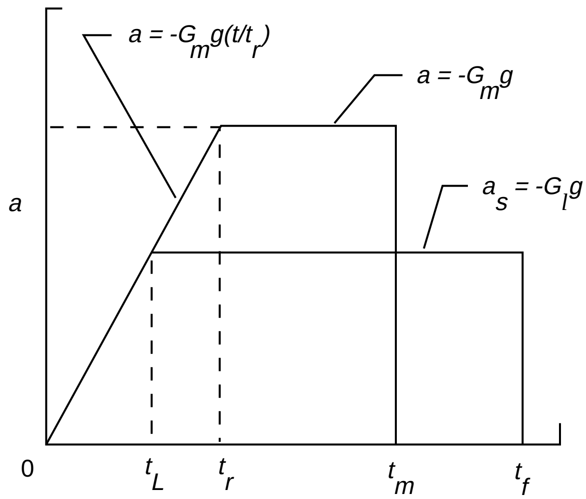


Sketch A

For aircraft structure, the velocity during the particular trapezoidal deceleration pulse can be expressed as

$$V_A = V_o + \int_0^t a\,dt \tag{1}$$

where $0 \le t \le t_r$, and substituting for $a$ (sketch A) gives

$$V_A = V_o + \int_0^t -G_m g \left(\frac{t}{t_r}\right) dt \tag{2}$$

Integrating equation (2) gives

$$V_A = V_o + \left[-G_m g \left(\frac{t^2}{2t_r}\right)\right]_0^t \tag{3}$$

which evaluates at $t = t_r$ to be

$$V_A = V_o - G_m g \frac{t_r}{2} \tag{4}$$

Equation (4) is the velocity history of the aircraft up to time $t_r$ of the trapezoidal crash loading. Using equation (3) now to determine the aircraft displacement as the integral of the velocity gives

$$S_A = \int_0^t V_A\,dt \tag{5}$$

or

$$S_A = \int_0^t \left(V_o - G_m g \frac{t^2}{2t_r}\right) dt \tag{6}$$

Integrating equation (6) gives

$$S_A = V_o t\Big]_0^t + G_m g \frac{t^3}{6t_r}\Big]_0^t \tag{7}$$

Evaluation at $t = t_r$ gives

$$S_A = V_o t_r - G_m g \frac{t_r^2}{6} \tag{8}$$

which is the general expression for the displacement of the aircraft up to time $t_r$ of the trapezoidal deceleration. For the time $t_r < t < t_m$,

$$V_A = V_o - G_m g \frac{t_r}{2} + \int_{t_r}^t -G_m g\,dt \tag{9}$$

Integrating and evaluating at $t = t_m$ for which $V_A = 0$ give

$$V_o = \left(\frac{G_m g}{2}\right)(2t_m - t_r) \tag{10}$$

Thus the total airplane displacement at $t = t_m$ is

$$S_A = V_o t_r - G_m g \frac{t_r^2}{6} + \int_{t_r}^{t_m} \left[V_o - G_m g \frac{t_r}{2} - G_m g(t - t_r)\right] dt \tag{11}$$

which integrates and evaluates in the limits to

$$S_A = V_o t_m - G_m g \frac{t_r^2}{6} - \left(G_m g \frac{t_m}{2}\right)(t_m - t_r) \tag{12}$$

For the seat/occupant, the total displacement is

$$S_S = \int_0^{t_L} V_{S,1}\,dt + \int_{t_L}^{t_f} V_{S,2}\,dt \tag{13}$$

where for $0 < t \le t_L$,

$$V_{S,1} = V_o + \int_0^t a\,dt \tag{14}$$

which evaluates within the limits, after substituting $a = -G_m g(t/t_r)$ and integrating, to be

$$V_{S,1} = V_o - G_m g \frac{t^2}{2t_r} \tag{15}$$

Additionally, for $t_L < t$,

$$V_{S,2} = \left[V_o + \int_0^t a\,dt\right] + \int_{t_L}^t a_s\,dt \tag{16}$$

which upon appropriate substitution of $a = -G_m g \times (t/tr)$ and $a_s = -G_l g$, integration, and evaluation within the limits is

$$V_{S,2} = V_o - G_m g \frac{t_L^2}{2t_r} - G_l g(t - t_L) \qquad (17)$$

and the total seat/occupant displacement is, in terms of equations (15) and (17),

$$S_S = \int_0^{t_L} \left( V_o - G_m g \frac{t^2}{2t_r} \right) dt + \int_{t_L}^{t_f} \left[ V_o - G_m g \frac{t_L^2}{2t_r} - G_l g(t - t_L) \right] dt \qquad (18)$$

Upon integration and evaluation of equation (18), the total seat/occupant displacement is found to be

$$S_S = V_o t_f + G_m g \frac{t_L^3}{3t_r} - G_m g \frac{t_L^2 t_f}{2t_r} - \frac{G_l g}{2}(t_f - t_L)^2 \qquad (19)$$

An equation for time $t_f$ is also required. Since at $t = t_f$, $V_{S,2} = 0$, equation (17) can be used to determine $t_f$. Thus, recalling $V_o$ from equation (10) and defining

$$K = \frac{t_L}{t_r} = \frac{G_l}{G_m}$$

and noting that

$$t_L = K t_r$$

give the solution for the time to be

$$t_f = \frac{1}{2} K \left[ 2(t_m + K t_L) - \frac{t_r^2 + t_L^2}{t_r} \right] \qquad (20)$$

For specific velocity changes and maximum $g$ of the trapezoidal pulse, time $t_m$ can be determined as

$$t_m = \frac{V_o}{G_m g} + \frac{t_r}{2} \qquad (21)$$

Since seat stroke is eventually desired, the seat/occupant displacement minus the airplane displacement gives the stroke of the seat or

$$S = \left[ V_o t_f + G_m g \frac{t_L^3}{3t_r} - G_m g \frac{t_L^2 t_f}{2t_r} - \frac{G_l g}{2}(t_f - t_L)^2 \right] - \left[ V_o t_m - G_m g \frac{t_r^2}{6} - G_m g \frac{t_m}{2}(t_m - t_r) \right] \qquad (22)$$

Derivation of similar equations for the other pulse loading shapes is not included; however, pertinent equations similar to those presented above for the trapezoidal pulse are included in the appendix. The equations allow seat strokes to be determined for the other pulse shapes.

## Results and Discussion

In figures 3 through 8, peak deceleration $G_m$ is plotted as a function of initial impact velocity $V_o$ or seat stroke $S$ for several chosen pulse durations $t_m$ or rise times $t_r$. A line is drawn vertically from an initial impact velocity (to be dissipated under the crash pulse) up to a desired pulse duration (or rise time) curve and extended horizontally to the value of the peak deceleration which would be necessary to achieve the velocity change. Where the horizontal line intersects the seat stroke curve (for the same pulse duration, or rise time), a vertical line is drawn to the abscissa to indicate what seat stroke would be *required to limit the deceleration to a 12g level on the seat pan.*

In discussing the results of the seat stroke requirements under the various pulse shape loadings, the velocity change of 31 ft/sec and rise time to peak deceleration of 0.05 or 0.06 sec (associated with Federal Regulations Part 23 for GA dynamic seat testing, ref. 14) are used as the reference point.

### Trapezoidal Pulse Loading

The first pulse shape considered is the trapezoidal pulse which is characterized by a sloped line rising to a peak value which remains constant until all the velocity involved in the impulse is removed. Figure 3(a) presents the peak deceleration and seat stroke data for the fixed rise time to a peak of 0.05 and 0.06 sec, respectively, with a fixed total pulse duration $t_m$ (computed from the peak deceleration of 19$g$, with a change in velocity of 31 ft/sec for the 0.05-sec rise time or from the peak deceleration of 15$g$ peak with a change in velocity of 31 ft/sec for the 0.06-sec rise time specified in Part 23). At the Part 23 requirement of change in velocity of 31 ft/sec, rise time to peak deceleration of 0.05 sec, a 19$g$ value is obtained. Likewise, for the 0.06-sec rise time, the 15$g$ peak is also possible. For these parameters, a seat stroke of 2.6 and 1.2 in., respectively, is indicated to maintain the load on the seat pan to a 12$g$ limit.

Additionally, in figure 3(b) with compressed scales, experimental peak decelerations at their respective velocity changes have been plotted for the general aviation aircraft tests which were conducted at the Langley Research Center. (See refs. 17 and 18.) With the exception of four data points, all the general aviation crash data lie outside the boundaries formed by the vertical line through the velocity change of 31 ft/sec and the horizontal line through the peak deceleration of $19g$. The indication is that the Part 23 test values relative to the simulated real world crash data can be termed as minimum requirements for the dynamic testing of general aviation seats. Since the results in figure 3(a) indicate stroking of the seats is required under the specified test parameters and since most data in figure 3(b) are higher in magnitudes than the stated requirements, seat stroking capability would be highly desirable to attempt to provide a measure of protection to occupants undergoing crash loads.

### Sine Pulse Loadings

***Half-sine pulse.*** Figure 4 presents peak deceleration as a function of velocity change for different pulse durations of the half-sine crash pulse along with the required seat stroke to achieve the reduced seat pan loading under the various assumed peak magnitudes of the half-sine crash pulse. For total pulse durations between 0.065 and 0.120 sec, corresponding to velocity changes of 16 to 30 ft/sec with a peak pulse magnitude of $12g$, no seat stroke would be required. However, for a vertical velocity change of 31 ft/sec with a 0.10-sec duration (rise time to peak = 0.05 sec) the seat would have to stroke approximately 1 in. at the design limit load ($12g$) to provide protection from the $15g$ maximum deceleration pulse loading. Note, however, that Part 23 requires a 0.06-sec rise time with the $15g$ peak input deceleration. Furthermore, the input magnitude of $19g$ is only possible with a pulse duration of approximately 0.081 sec (Rise time = 0.0405 sec, not the required 0.05 sec). Seat stroke for the $19g$ pulse is about 3 in. If the pulse duration were 0.065 sec, the deceleration peak is $23g$ and a seat stroke of about 4.5 in. would be necessary for occupant protection.

***Quarter-sine pulse.*** Figure 5 presents the deceleration and stroke results for the quarter-sine pulse loading. As expected, the data are not dramatically different from the half-sine pulse loading discussed in the previous section. Similarly, the Part 23 parameters of velocity change of 31 ft/sec with a time to peak deceleration of 0.05 sec cannot be fulfilled with this particular shape. For example, a peak value of $19g$ with a velocity change of 31 ft/sec requires a total duration of 0.081 sec (which is also the rise time to peak) of the quarter-sine pulse, whereas the specification is 0.05 sec. With a pulse magnitude of $15g$ with velocity change of 31 ft/sec, the duration is 0.1 sec, and for the 0.05-sec pulse at velocity change of 31 ft/sec, just over $30g$ is indicated which is much too high a peak loading compared with the peak of $19g$ stated in the Part 23 specification. At the loading of $30g$, about 5.4 in. of seat stroke is indicated.

### Triangular Pulse Loadings

The following sections discuss the triangular-shaped pulses, the skewed and the symmetrical, relative to the effect that shape has on seat stroke and occupant response under dynamic loads. The triangular pulse was found to approximate well the actual crash pulses measured during the GA Crash Dynamics Program. (See refs. 17 and 18.) For the study of this paper, one nonsymmetrical pulse and one symmetrical triangular pulse were selected. The difficulty of generating and controlling the drop-off of triangular pulse shapes in a laboratory is one reason that the Part 23 regulation specifies only the peak deceleration and rise time to peak with a velocity change rather than a total pulse shape. Generating such parameters is easier in a laboratory if the form is a trapezoidal pulse shape, and additionally, both requirements of Part 23 can be readily achieved with such a shape.

***Skewed triangle.*** Data for the skewed triangular loading pulse are presented in figure 6. With the velocity change of 31 ft/sec of Part 23, a pulse duration of 0.1 sec essentially gives the peak deceleration of $19g$; however, the curves in figure 6 are for a rise time to the peak deceleration being 7/8 of the total pulse duration or for the 0.1-sec pulse duration under consideration, 0.088 sec. Therefore, the pulse gives, as stated, approximately the correct velocity change and the peak deceleration but does not provide the desired rise time to peak deceleration. Although this particular skewed triangular loading does not provide all the desired test parameters for seat testing under Part 23, it does indicate that at a velocity change of 31 ft/sec, 0.1 sec, and a peak deceleration of $19g$, about 1 in. of seat stroke should be provided to limit the load on the seat pan to the design limit of $12g$.

***Symmetric triangle.*** For the triangular shape where the rise time is half the total pulse duration, a symmetric triangular loading exists. Figure 7(a) presents peak deceleration and seat stroke data for the symmetric triangular loading pulse shape. For a pulse duration of 0.1 sec (rise time of 0.05 sec) and a velocity change of 31 ft/sec, the peak deceleration of 19$g$ is achieved, and approximately 0.5 in. of seat stroke would be necessary to limit the loads on the seat pan to the limit of 12$g$ which is being used in all the examples of this paper. For comparison, experimental crash pulse data are included with the trapezoidal pulse and are also shown on compressed scales in figure 7(b). The primary emphasis of this plot is, therefore, that the parameters suggested for the testing of seats under dynamic inputs as contained in the Part 23 regulations are "minimum requirements" relative to the crash data from full-scale aircraft tests. A second point is that, even under what has been stated to be a minimum requirement, seat stroking capability for the protection of seat occupants is strongly suggested from the data of figure 7 as well as the other pulse shapes included in this paper.

### Trapezoids and Triangles

It should be noted that a skewed triangular pulse with a rise time of 0.06 sec and total pulse duration of 0.128 sec can provide the peak deceleration of 15$g$ and velocity change of 31 ft/sec as specified by Part 23. However, as mentioned previously, practical considerations such as the difficulty of generating and controlling the drop-off of triangular pulse shapes led the GASP panel to recommend that the requirement be stated as peak loads, times, and velocity changes with the unstated being that a trapezoidal type pulse that can be achieved in a laboratory could fulfill the stated requirements.

A question may arise "How do the responses under the trapezoidal pulse inputs compare with triangular pulses which were found to approximate closely the actual crash pulses in the GA testing?" Figure 8 shows a comparison of a triangular and a trapezoidal pulse with rise time of 0.05 sec and a triangular and a trapezoidal pulse with rise time of 0.06 sec. It may be noted that the trapezoidal pulses (open symbols) *are conservative*, since they require slightly more stroke in the seat to limit the loads on the seat pan than the comparable triangular pulses (closed symbols). For example, the 0.05-sec trapezoidal pulse at 19$g$, velocity change of 31 ft/sec, requires a seat stroke of about 2.5 in., whereas the 0.1-sec triangular pulse requires only about 1.5 in. Similarly, the 0.06-sec trapezoidal pulse requires just over 1 in. of stroke, whereas the 0.128-sec triangular pulse requires no stroke. Thus, the trapezoidal pulse which is easier to generate experimentally provides some conservatism in the tests, which is a desirable situation. This is especially good since it has been shown that the stated *peak decelerations and velocity change of the requirements are generally below the actual aircraft crash test results* (see figs. 3(b) and 7(b)).

### Response Considerations of Dummy Occupant

Data relative to the response behavior of the dummy occupant under controlled inputs are presented in figures 9 and 10. As noted in reference 17, the DRI is one of several means often used for assessing potential responses of occupants to crash inputs. Although the DRI is a simple model (fig. 9), it introduces into consideration dynamic response under crash pulse inputs. If, for example, the resulting 12$g$ controlled trapezoidal limit load pulse on the seat pan location (resulting from the trapezoidal and symmetrical triangular input crash pulses of the present study) is used as an input to the DRI model, direct computations indicate the response to be a DRI of about 17.2$g$. The impulse or product of the 12$g$ maximum load on the seat pan (and input to the occupant) and time $G_l t_f$ (1.2 to 1.3 sec for the trapezoidal and symmetrical triangular input pulses) can be related to the DRI. For instance, in figure 10 (which is a plot of normalized DRI response as a function of the impulse, ref. 17), the response at the 1.2 impulse value is in a region that amplifies by approximately 1.4 the essentially trapezoidal input pulse that the occupant experiences at the seat pan. Thus the 12$g$ level translates to a DRI in the occupant of approximately 17$g$ from figure 10 which was also verified by direct computations of DRI.

In reference 16, the test results of both energy-absorbing and non-energy-absorbing seats were obtained under application of Part 23 input pulse. Pelvic forces as a function of DRI were monitored in the tests series and a DRI of approximately 19$g$ was found to correlate with 1500 lbf in the pelvis of the dummy occupant. Such results would indicate that (since seat stroke was included in the present study) the 17$g$ DRI is probably a fairly good estimate of the value that would be experienced by the dummy with control of the load on the seat pan to the 12$g$ level, and consequently, the 1500 lbf pelvic force level would likely not be exceeded. Additionally, such results further emphasize the need for designed seat stroking to provide for some occupant protection in crash situations.

## Conclusions

An analytical study has been made of the effects of pulse shape models (which potentially could be used to simulate actual crash pulses) on the required stroking of aircraft seats to maintain a design limit load on the seat pan during the particular crash pulse application. Equations for five assumed shapes of crash pulse loadings were derived to express the displacement of the aircraft structure and the displacement of the seat/occupant in terms of the maximum deceleration, velocity change, limit seat load, and pulse time. Seat stroke data were computed under test conditions as specified in Part 23 § 23.562(b)(1) for dynamic testing of general aviation seats. An examination of the results and a comparison of the data to full-scale crash test data for aircraft indicated the following conclusions:

1. One pulse, the trapezoidal, was capable of providing the required parameters of both test conditions specified in the Part 23 § 23.562(b)(1) regulation.

2. The symmetrical triangle was capable of providing only the required parameters of the highest input pulse specified in the Part 23 § 23.562(b)(1) regulation.

3. The half-sine, quarter-sine, and one specific skewed triangular pulse could not provide the required inputs for seat testing specified in the Part 23 § 23.562(b)(1) regulation.

4. Adjustments in the skew of the triangular pulse to provide a rise time of 0.06 sec with a total pulse duration of 0.128 sec would permit the skewed triangle to provide the necessary peak $g$ level and velocity change only for the lower input pulse requirement of the Part 23 § 23.562(b)(1) regulation.

5. Essentially all five different pulse shapes at or near the Part 23 § 23.562(b)(1) regulation of 19$g$ occurring at 0.05 sec, or 15$g$ occurring at 0.06 sec with a velocity change of 31 ft/sec, require seat stroke to limit the loads on the seat pan (and consequently on the occupant) to a design limit below the peak input value.

6. A comparison of the specified seat test parameters of the Part 23 regulation with full-scale crash test data from the NASA General Aviation Crash Test Program indicated that the required test conditions can be readily termed a minimum requirement for the testing of general aviation seats.

NASA Langley Research Center
Hampton, VA 23665-5225
December 19, 1991

## Appendix

## Equations for Evaluating Seat Stroke Requirements for Different Pulse Loading Shapes

Presented in this appendix are the equations for evaluating the seat stroke requirements for pulse loading shapes which include the half-sine, quarter-sine, skewed triangular, and symmetrical triangular pulses. The detailed derivation is not included, but the steps are essentially identical to those for the trapezoidal pulse in the main text.

### Sine Pulse Loadings

***Half-sine.*** Sketch B illustrates the half-sine pulse-loading shape. The equations for evaluating the seat stroke requirements follow the sketch.

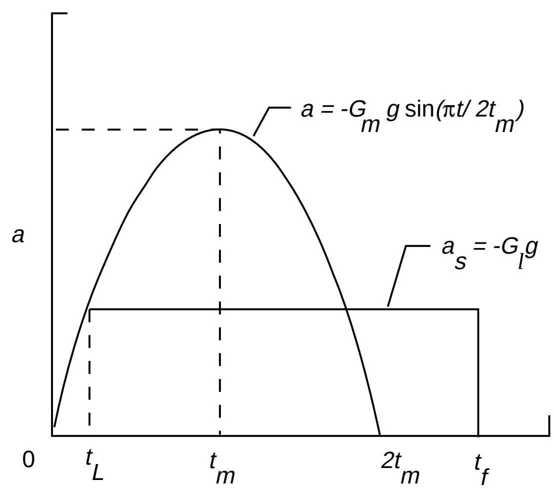


Sketch B

Initial impact velocity:

$$V_o = \frac{4G_m g t_m}{\pi} \tag{A1}$$

Displacement of aircraft:

$$S_A = 2V_o t_m - \frac{4G_m g t_m^2}{\pi} \tag{A2}$$

Seat/occupant displacement:

$$\begin{aligned} S_S = V_o t_L &- \frac{2G_m g t_m t_L}{\pi} + \frac{4G_m g t_m^2}{\pi^2} \sin \frac{\pi t_L}{2t_m} \\ &+ V_o(t_f - t_L) - \frac{2G_m g t_m}{\pi} \\ &\times \left(1 - \cos \frac{\pi t_L}{2t_m}\right)(t_f - t_L) \\ &- \frac{G_l g}{2}(t_f^2 - t_L^2) + G_l g t_L (t_f - t_L) \end{aligned} \tag{A3}$$

Ratio of limit load to peak deceleration:

$$K = \frac{G_l}{g_m} = \sin\left(\frac{\pi t_L}{2t_m}\right) \tag{A4}$$

Time to reach limit seat deceleration:

$$t_L = \left(\frac{2}{\pi} \sin^{-1} K\right) t_m \tag{A5}$$

Total seat/occupant pulse duration:

$$\begin{aligned} t_f = \Bigg\{ &\frac{4}{\pi}\frac{1}{K} - \frac{2}{\pi}\left[1 - \cos(\sin^{-1} K)\ \frac{1}{K}\right] \\ &+ \frac{2}{\pi} \sin^{-1} K \Bigg\} t_m \end{aligned} \tag{A6}$$

Seat stroke:

$$\begin{aligned} S = V_o t_L &- \frac{2G_m g t_m t_L}{\pi} \\ &+ \frac{4G_m g t_m^2}{\pi^2} \sin \frac{\pi t_L}{2t_m} + V_o(t_f - t_L) \\ &- \frac{2G_m g t_m}{\pi}\left(1 - \cos \frac{\pi t_L}{2t_m}\right)(t_f - t_L) \\ &- \frac{G_l g}{2}(t_f^2 - t_L^2) + G_l g t_L (t_f - t_L) \\ &- \left(2V_o t_m - \frac{4G_m g t_m^2}{\pi}\right) \end{aligned} \tag{A7}$$

***Quarter-sine.*** The equations for the quarter-sine crash pulse loading and sketch C that illustrates the quarter-sine pulse are presented as follows:

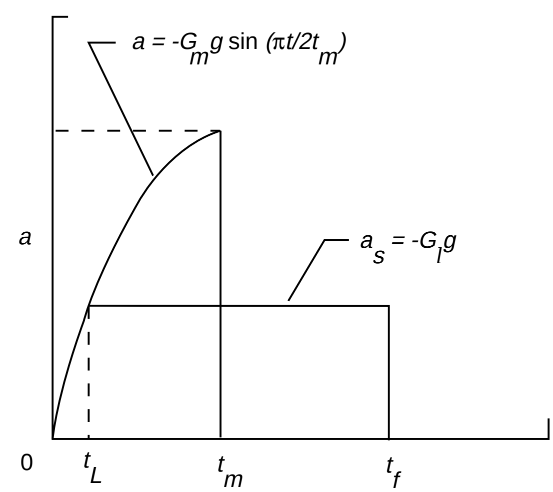


Sketch C

Initial impact velocity:

$$V_o = \frac{2G_m g t_m}{\pi} \qquad \text{(A8)}$$

Displacement of aircraft:

$$S_A = \frac{4G_m g t_m^2}{\pi^2} \qquad \text{(A9)}$$

Seat/occupant displacement:

$$\begin{aligned} S_S = {} & V_o t_L - \frac{2G_m g t_m t_L}{\pi} + \frac{4G_m g t_m^2}{\pi^2} \sin \frac{\pi t_L}{2t_m} \\ & + V_o(t_f - t_L) - \frac{2G_m g t_m}{\pi} \\ & \times \left(1 - \cos \frac{\pi t_L}{2t_m}\right)(t_f - t_L) - \frac{G_l g}{2}(t_f^2 - t_L^2) \\ & + G_l g t_L (t_f - t_L) \end{aligned} \qquad \text{(A10)}$$

Ratio of limit load to peak deceleration:

$$K = \frac{G_l}{G_m} = \sin \frac{\pi t_L}{2t_m} \qquad \text{(A11)}$$

Time to reach limit seat deceleration:

$$t_L = \left(\frac{2}{\pi} \sin^{-1} K\right) t_m \qquad \text{(A12)}$$

Total seat/occupant pulse duration:

$$t_f = \frac{2t_m}{\pi}\left[\frac{1}{K} \cos(\sin^{-1} K) + \sin^{-1} K\right] \qquad \text{(A13)}$$

Seat stroke:

$$\begin{aligned} S = {} & \Bigg[ V_o t_L - \frac{2G_m g t_m t_L}{\pi} + \frac{4G_m g t_m^2}{\pi^2} \sin \frac{\pi t_L}{2t_m} \\ & + V_o(t_f - t_L) - \frac{2G_m g t_m}{\pi}\left(1 - \cos \frac{\pi t_L}{2t_m}\right)(t_f - t_L) \\ & - \frac{G_l g}{2}\left(t_f^2 - t_L^2\right) + G_l g t_L (t_f - t_L) \Bigg] \\ & - \frac{4G_m g t_m^2}{\pi^2} \end{aligned} \qquad \text{(A14)}$$

**Triangular Pulse Loadings**

Equations for the skewed triangular pulse loading and the symmetrical triangle, which is a special case of the skewed shape, are presented. Sketch D illustrates the skewed triangular pulse loading shape; sketch E, the symmetrical triangle.

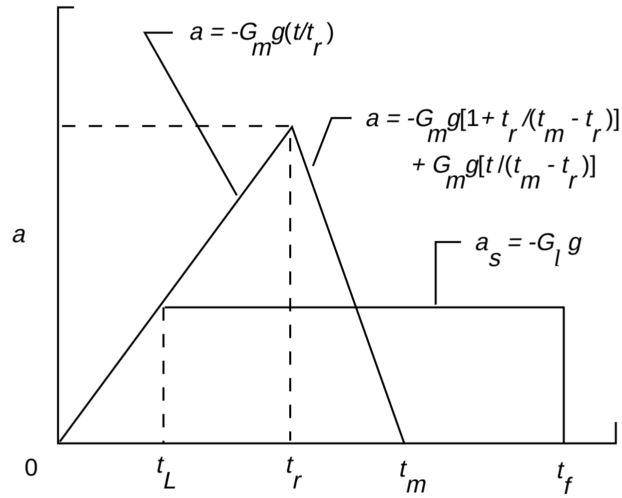


Sketch D

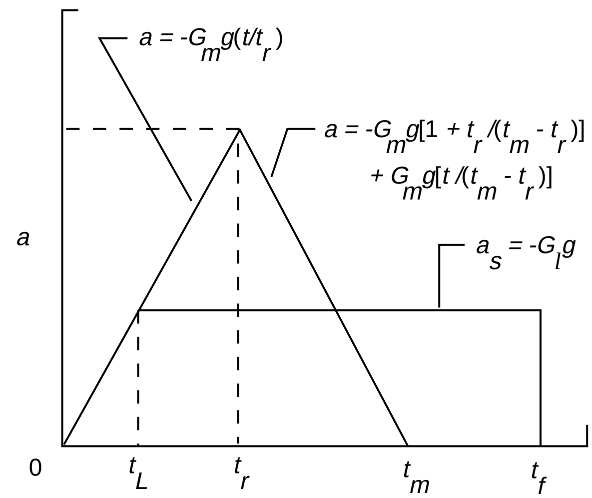


Sketch E

Initial impact velocity:

$$V_o = \frac{G_m g t_m}{2} \qquad \text{(A15)}$$

Displacement of aircraft:

$$\begin{aligned} S_A = {} & V_o t_m - \frac{G_m g t_r^2}{6} - \frac{G_m g t_r}{2}(t_m - t_r) \\ & - \frac{1}{2}\frac{G_m g t_m}{t_m - t_r}\left(t_m^2 - t_r^2\right) + G_m g t_m t_r \\ & - \frac{G_m g t_r^2}{2} + \frac{G_m g}{6(t_m - t_r)}(t_m^3 - t_r^3) \end{aligned} \qquad \text{(A16)}$$

Seat/occupant displacement:

$$S_S = V_o t_f + \frac{G_m g t_L^3}{3t_r} - G_m g(t_L^2)\frac{t_f}{2t_r} - \frac{G_l g}{2}(t_f - t_L)^2 \qquad \text{(A17)}$$

Ratio of limit load to peak deceleration:

$$K = \frac{G_l}{G_m} \qquad \text{(A18)}$$

Time to reach limit seat deceleration:

$$\left.\begin{aligned} t_L &= K\left(\tfrac{7}{8}\right)t_m \quad \text{(Skewed)} \\ t_L &= \left(\tfrac{K}{2}\right)t_m \quad \text{(Symmetrical)} \end{aligned}\right\} \qquad \text{(A19)}$$

(7/8 has been assumed for the skewed triangle, whereas 1/2 is used for the symmetrical triangle).

Total seat/occupant pulse duration:

$$t_f = \frac{t_m}{2}\left(\frac{1}{K} + \frac{7}{8}K\right) \qquad \text{(A20)}$$

thus,

$$\begin{aligned} S = &\left[V_o t_f + \frac{G_m g t_L^3}{3t_r} - G_m g\left(t_L^2\right)\frac{t_f}{2t_r}\right. \\ &\left. - \frac{G_l g}{2}(t_f - t_L)^2\right] \\ &- \left[V_o t_m - \frac{G_m g t_r^2}{6} - \frac{G_m g t_r}{2}(t_m - t_r)\right. \\ &- \frac{1}{2}\frac{G_m g t_m}{t_m - t_r}\left(t_m^2 - t_r^2\right) + G_m g t_m t_r \\ &\left. - \frac{G_m g t_r^2}{2} + \frac{G_m g}{6(t_m - t_r)}(t_m^3 - t_r^3)\right] \end{aligned} \qquad \text{(A21)}$$

## References


1. De Haven, Hugh: Causes of Injury in Lightplane Accidents. *Aero Dig.,* vol. 44, no. 5, Mar. 1, 1944, pp. 51–55, 206.

2. Hasbrook, A. Howard: What a Spray Plane Should Have. *Aviation Week,* vol. 52, no. 7, Feb. 13, 1950, pp. 25–27, 30–31.

3. Hoekstra, Harold D.; and Huang, Shung-Chai: *Safety in General Aviation.* Flight Safety Found., Inc., 1971.

4. Eiband, A. Martin: *Human Tolerance to Rapidly Applied Accelerations: A Summary of the Literature.* NASA MEMO 5-19-59E, 1959.

5. Pinkel, I. Irving; and Rosenberg, Edmund G.: *Seat Design for Crash Worthiness.* NACA Rep. 1332, 1957. (Supersedes NACA TN 3777.)

6. Fasanella, Edwin L.; and Alfaro-Bou, Emilio: NASA General Aviation Crashworthiness Seat Development. [Preprint] 790591, Soc. of Automotive Engineers, Apr. 1979.

7. Svoboda, Craig M.; and Warrick, James C.: *Design and Development of Variable-Load Energy Absorbers.* Rep. No. NADC-80257-60, U.S. Navy, June 1981. (Available from DTIC as AD A103 206.)

8. Alfaro-Bou, Emilio; Fasanella, Edwin L.; and Williams, M. Susan: Crashworthy Design Considerations for General Aviation Seats. SAE Tech. Paper Ser. 850855, Apr. 1985.

9. Eichelberger, Charles P.; Alfaro-Bou, Emilio; and Fasanella, Edwin L.: Development of an Energy-Absorbing Passenger Seat for a Transport Aircraft. *19th Aerospace Mechanisms Symposium,* NASA CP-2371, 1985, pp. 39–58.

10. Shane, S. Joseph: *Design and Testing of an Energy-Absorbing Crewseat for the F/FB-111 Aircraft. Volume I—Final Report.* NASA CR-3916, 1985.

11. Shane, S. Joseph: *Design and Testing of an Energy-Absorbing Crewseat for the F/FB-111 Aircraft. Volume II—Data From Seat Testing.* NASA CR-3917, 1985.

12. Shane, S. Joseph: *Design and Testing of an Energy-Absorbing Crewseat for the F/FB-111 Aircraft. Volume III—Data From Crew Module Testing.* NASA CR-3918, 1985.

13. Soltis, Stephen J.; and Olcott, John W.: The Development of Dynamic Performance Standards for General Aviation Aircraft Seats. SAE Tech. Paper Ser. 850853, Apr. 1985.

14. Small Airplane Airworthiness Review Program, Amendment No. 1; Final Rule—14 CFR, Part 23. *Fed. Regist.,* vol. 53, no. 157, Aug. 15, 1988, pp. 30802–30815.

15. Payne, Peter R.; and Stech, Ernest L.: *Dynamic Models of the Human Body.* AMRL-TR-66-157, U.S. Air Force, Nov. 1969. (Available from DTIC as AD 701 383 and also available as NASA TM X-67038.)

16. Chandler, Richard F.: Data for the Development of Criteria for General Aviation Seat and Restraint System Performance. *Crash Dynamics of General Aviation Aircraft,* SP-622, Soc. of Automotive Engineers, Inc., 1985, pp. 13–28. (Available as SAE Paper 850851.)

17. Carden, Huey D.: *Correlation and Assessment of Structural Airplane Crash Data With Flight Parameters at Impact.* NASA TP-2083, 1982.

18. Carden, Huey D.: Impulse Analysis of Airplane Crash Data With Consideration Given to Human Tolerance. SAE Tech. Paper Ser. 830748, Apr. 1983.

# REPORT DOCUMENTATION PAGE

*Form Approved*
*OMB No. 0704-0188*



**1. AGENCY USE ONLY** *(Leave blank)*

**2. REPORT DATE**
February 1992

**3. REPORT TYPE AND DATES COVERED**
Technical Paper

**4. TITLE AND SUBTITLE**
Effect of Crash Pulse Shape on Seat Stroke Requirements for Limiting Loads on Occupants of Aircraft

**5. FUNDING NUMBERS**
WU 505-63-50-09

**6. AUTHOR(S)**
Huey D. Carden

**7. PERFORMING ORGANIZATION NAME(S) AND ADDRESS(ES)**
NASA Langley Research Center
Hampton, VA 23665-5225

**8. PERFORMING ORGANIZATION REPORT NUMBER**
L-16941

**9. SPONSORING/MONITORING AGENCY NAME(S) AND ADDRESS(ES)**
National Aeronautics and Space Administration
Washington, DC 20546-0001

**10. SPONSORING/MONITORING AGENCY REPORT NUMBER**
NASA TP-3126

**11. SUPPLEMENTARY NOTES**

**12a. DISTRIBUTION/AVAILABILITY STATEMENT**

Unclassified–Unlimited

Subject Category 39

**12b. DISTRIBUTION CODE**

**13. ABSTRACT** *(Maximum 200 words)*
An analytical study was made to (1) provide comparative information on various crash pulse shapes that potentially could be used to test seats under conditions included in Federal Regulations Part 23 § 23.562(b)(1) for dynamic testing of general aviation seats, (2) show the effects that crash pulse shape can have on the seat stroke requirements necessary to maintain a specified limit loading on the seat/occupant during crash pulse loadings, (3) compare results from certain analytical model pulses with approximations of actual crash pulses, and (4) compare analytical seat results with experimental airplane crash data. Structural and seat/occupant displacement equations in terms of the maximum deceleration, velocity change, limit seat pan load, and pulse time for five potentially useful pulse shapes were derived; from these, analytical seat stroke data were obtained for conditions as specified in Federal Regulations Part 23 § 23.562(b)(1) for dynamic testing of general aviation seats.

**14. SUBJECT TERMS**
Crashworthiness; Crash dynamics; Human tolerance; General aviation seats; Seat testing

**15. NUMBER OF PAGES**
21

**16. PRICE CODE**
A03

| 17. SECURITY CLASSIFICATION OF REPORT | 18. SECURITY CLASSIFICATION OF THIS PAGE | 19. SECURITY CLASSIFICATION OF ABSTRACT | 20. LIMITATION OF ABSTRACT |
|---|---|---|---|
| Unclassified | Unclassified | | |

NSN 7540-01-280-5500

**Standard Form 298 (Rev. 2-89)**
Prescribed by ANSI Std. Z39-18
298-102

NASA-Langley, 1992